

# Intra-Variable Handwriting Inspection Reinforced with Idiosyncrasy Analysis

Chandranath Adak, *Member, IEEE*, Bidyut B. Chaudhuri, *Life Fellow, IEEE*,  
Chin-Teng Lin, *Fellow, IEEE*, and Michael Blumenstein, *Senior Member, IEEE*

**Abstract**—In this paper, we work on intra-variable handwriting, where the writing samples of an individual can vary significantly. Such within-writer variation throws a challenge for automatic writer inspection, where the state-of-the-art methods do not perform well. To deal with intra-variability, we analyze the idiosyncrasy in individual handwriting. We identify/verify the writer from highly idiosyncratic text-patches. Such patches are detected using a deep recurrent reinforcement learning-based architecture. An idiosyncratic score is assigned to every patch, which is predicted by employing deep regression analysis. For writer identification, we propose a deep neural architecture, which makes the final decision by the idiosyncratic score-induced weighted sum of patch-based decisions. For writer verification, we propose two algorithms for deep feature aggregation, which assist in authentication using a triplet network. The experiments were performed on two databases, where we obtained encouraging results.

**Index Terms**—Deep Learning, Idiosyncratic Writing, Intra-variable Handwriting, Reinforcement Learning, Writer Identification, Writer Verification.

## I. INTRODUCTION

Handwriting is still considered as strong evidence in criminal courts of many countries due to its solid impact on behavioral biometrics [1]. Therefore, for the last four decades, research on handwriting inspection has been of great interest in forensics. Moreover, the computational approaches are embedded in handwriting forensics owing to booming automation since the late 20<sup>th</sup> century. Besides, the “9/11” and “2001 anthrax” attacks have reignited the computational handwriting forensics research [23].

From the forensic perspective, the handwritten specimen can mostly be found as an offline sample in the form of a threat letter, suicide note, forged manuscript, etc. Therefore, in this paper, we focus on offline handwriting. The offline handwriting analysis is more challenging compared to online writing due to the absence of stroke trajectory, writing pressure, velocity, etc.

In computational handwriting analysis, the focus during the last decade and the first half of the current decade were on handcrafted features. The deep neural net derived feature-based works have thrived during the latter half of the current decade [2]. Although the past researches on writer inspection have

produced some encouraging results, their major works have been performed on inter-variable writing [22]. The research on intra-variability of handwriting has been somewhat overlooked. However, handwriting intra-variability is observed rather frequently due to some mechanical, physical, and psychological factors of the writers [10]. To the best of our knowledge, only one computational experiment has been performed on intra-variability due to Adak et al. [10]. In that study, they experimentally showed that the general handcrafted and deep feature-based models did not work well on intra-variable writer inspection, i.e., training/testing on disparate writing styles. Now, our paper comes into place to inspect the writer on intra-variable handwriting due to having practical concerns [10]. For this purpose, the idiosyncrasy analysis [3] of handwriting may be useful.

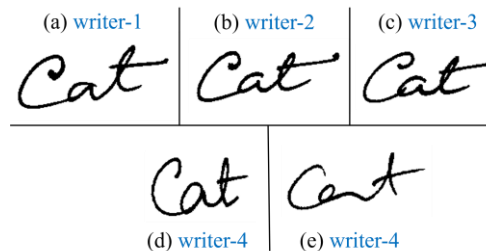


Figure 1. (a), (b), (c): 3 samples written by 3 different writers: low Inter-variability; (d), (e): 2 samples written by the same writer: high Intra-variability.

In Figure 1, we present some examples concerning intra-variable and inter-variable handwriting. The samples of the upper row (Figure 1. (a)-(c)) seem to be structurally similar; however, these are written by three different writers. It depicts the *low inter-variability*. Such low inter-variability is mostly seen during the intention of writing/signature forgery [24]. Here, writer-2 (Figure 1. (b)) and writer-3 (Figure 1. (c)) forge the inscription of writer-1 (Figure 1. (a)). In Figure 1. (a), (b), two writing samples look to be dissimilar, but both written by the same writer, i.e., writer-4. It portrays *high intra-variability*. In this paper, we are concerned with such high intra-variability in contrast with the past works [22, 23].

Idiosyncrasy analysis of handwriting refers to examining the eccentricity in individual writing style [3]. We observe that

C. Adak is with the School of Computer Science, FEIT, University of Technology Sydney, Australia-2007, and Centre for Data Science, JIS Institute of Advanced Studies and Research, JIS University, India-700091.

B.B. Chaudhuri is with Techno India University, India-700091, and CVPR Unit, Indian Statistical Institute, India-700108.

C.T. Lin and M. Blumenstein are with the Centre for AI, School of Computer Science, FEIT, University of Technology Sydney, Australia-2007. (e-mail: adak32@gmail.com, Chandranath.Adak@uts.edu.au).

almost every writer scribbles some character-texts in a peculiar style, which may be useful to inspect the writer on intra-variable writing. In *Figure 2*, we present two examples in English and Bengali scripts, where the writing idiosyncrasy is marked by red dashed boxes. Usually, to write the English character ‘d’, at first the lower loop is scribbled, then the vertical straight line is drawn. However, in *Figure 2.(a)*, to write ‘d’, the vertical line is penned before the loop creation. Therefore, here, instead of the lower part (loop), the upper part (vertical line) of the ‘d’ creates a continuity with the previous character, which represents the individual idiosyncrasy. In *Figure 2.(b)*, to write the Bengali character ‘ঈ’, an unnecessary ink-stroke gap makes the character penning highly idiosyncratic.

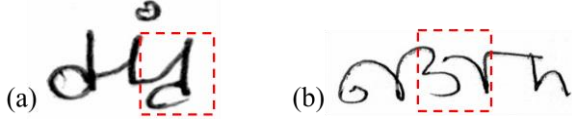


*Figure 2. Idiosyncratic writing samples in (a) English and (b) Bengali scripts, marked in red dashed boxes.*

In [3], a preliminary work on idiosyncrasy analysis is performed, which did not deal with intra-variable writing; however, it provided an insight that such analysis has a positive impact on writer identification. Adak et al. [3] modeled the idiosyncrasy analysis task into a classification problem to classify the text-patches into multiple classes defined by an idiosyncratic score. Their patch selection is mostly based on a sequential search with character-level information. In the current paper, we formulate the idiosyncrasy analysis task in a more sophisticated way, where we predict the idiosyncratic score through the deep regression [25], and select highly idiosyncratic patches using reinforcement learning [5].

Now, we inspect the writer from these idiosyncratic patches, instead of using all the patches, that was performed in [10]. The writer inspection is a task to examine a handwritten document. In this paper, the examination involves the identification and verification of a writer [10]. In the writer identification task, we find the correct writer-id of a questioned handwritten sample from multiple samples of different writers of a database. As a matter of fact, writer identification is a multi-class classification problem, where we need to find an unknown writer class among multiple writer classes [10]. In the writer verification task, we authenticate an asked handwriting sample whether it has been written by a particular writer or not. Therefore, writer verification is a binary classification problem [10]. For writer identification and verification, we use some deep-learning-based features. We perform the experiment on the database used in [10], which contains relatively high intra-variable Bengali offline handwriting. The outcome of our method is better than that presented in [10].

Among multiple applications of such research as mentioned in [10], the major one is inspecting a writer when a particular type of writing style of an individual is absent during training. The state-of-the-art methods do not perform well in such a case.

The *contributions* of our research are briefly mentioned as follows:

(i) The state-of-the-art methods including [10] did not perform

so well to inspect the writer on highly intra-variable handwriting. The method proposed in this paper performs better than past methods. Merging the idiosyncrasy analysis with intra-variable handwriting for writer inspection is newly proposed here.

(ii) We find highly idiosyncratic patches, and perform writer inspection on these patches only. To put an idiosyncratic score on a patch, we use a deep-feature induced regression analysis [25]. For highly idiosyncratic patch selection, we employ reinforcement learning [5]. In reinforcement learning, we propose a novel internal reward shaping function which is computed using the idiosyncratic score.

(iii) For writer identification, combining the decisions obtained from individual patches is a new contribution, where the overall decision is made by the idiosyncratic score-fed weighted sum of the individual patch-based decisions.

(iv) For writer verification, we propose two separate methods (MAF and XAF) for generating a combined page-level deep feature from multiple patch-level features.

The rest of the paper is organized as follows. Section II discusses our proposed method for idiosyncrasy analysis. Then Sections III and IV describe our writer identification and verification methods. The following Section V is about the experiments and results on our proposed methods. Finally, Section VI concludes this paper.

## II. IDIOSYNCRASY ANALYSIS

In this section, we perform idiosyncrasy analysis, whose objective is to find some highly idiosyncratic patches from a handwritten text sample, which can assist in writer inspection.

### A. Idiosyncratic Opinion Score

Before finding the highly idiosyncratic patches, we need to define an idiosyncrasy measure, based on which we can mark the respective patches as high or low. We adopt the idea of [3] to define this measure, i.e., subjective opinion score [19]. Now, we discuss the procedure to obtain the ground-truth score.

For ground-truthing, on a given text-patch ( $p_i$ ), multiple human handwriting experts provided their opinion scores ( $I_j^{(t)}$ ) within a continuous range of  $[I_L, I_H]$ ;  $I_L, I_H \in \mathbb{R}^+$ . Here, we choose  $I_L = 0, I_H = 10$ . The arithmetic mean ( $I_\mu^{(t)}$ ) of these scores is the *idiosyncratic opinion score* of a patch  $p_i$ .  $I_\mu^{(t)} = \frac{1}{e} \sum_{j=1}^e I_j^{(t)}$ ; where  $e > 1$  is the total count of experts that put score on a patch  $p_i$ . For our task,  $e \geq 30$ , i.e., at least 30 experts put individual scores on a patch. Adak et al. [3] partitioned the score range  $[I_L, I_H]$  into  $n_l$  number of bins (classes) of equal width and modeled a classification task to find highly idiosyncratic patch classes. Here, we approach differently by using regression analysis, where we predict the idiosyncratic score of a patch. In this paper, the score interval  $[I_L, I_H]$  is normalized into  $[0, 1]$  to produce normalized idiosyncratic score  $i_t$  of patch  $p_i$ , i.e.,  $i_t = \frac{I_\mu^{(t)} - I_L}{I_H - I_L}$ ;  $0 \leq i_t \leq 1$ . A patch  $p_i$  with  $i_t = 1$  refers to the highest idiosyncratic patch, whereas  $i_t = 0$  refers to the lowest one. As a matter of fact, on a page, multiple

patches with the same idiosyncratic score may present. This score ( $i_t$ ) assists in automated detection of highly idiosyncratic patches, as well as in writer inspection, in the following subsections.

### B. Detecting Idiosyncratic Patches

A handwritten page is scanned to be used as an input image. Now, the task is to detect the idiosyncratic patches from the input image. We consider the problem as a decision process where an agent interacts with a visual environment, viz., scanned handwritten page, to detect the target patches. Here, at each timestep (iteration), the agent partially observes the input image and decides where to focus on the next timestep.

We cast this problem as a partially observable Markov Decision Process (MDP) since it allows the agent to make a decision through stochastic control in discrete time and the entire environment is unobserved by the agent in a particular step [5]. Here, we employ a reinforcement learning-based agent which take action to learn a policy for maximizing reward [5]. The agent takes input of the state of current image status. MDP consists of a set of components, i.e., set of states of the current environment, set of actions to achieve the goal, reward to optimize decision strategy.

In this paper, the agent’s task is to find a patch from a handwritten page that can be used for writer inspection. Here, the agent will learn the policy through reinforcement learning to find the highly idiosyncratic patches.

In a handwritten page, a text-patch ( $p$ ) is a  $w_p \times w_p$  square box centering at a location  $l$  which is encoded with co-ordinate  $(x,y)$ . The co-ordinate  $(x,y)$  of the whole page image is ranged between  $(0,0)$  and  $(1,1)$ , where the top-left co-ordinate of the page is  $(0,0)$  and bottom-right is  $(1,1)$ .

From a patch, we extract some deep neural network-based features. Here, we use the ResNet-50 model for feature extraction since it achieved human-alike performance on ImageNet data [13]. Also, the skip connection concept of ResNet (*Residual Network*) makes the computation faster compared to some other deep architectures, such as VGG [4]. The ResNet takes a fixed size input of  $224 \times 224$ . Therefore, for our task also, we fix the  $w_p$  equals to 224. In Figure 3,  $f_g$  is actually a ResNet-50. Here, after the *avg pool* layer of ResNet-50 [4], we obtain a 2048-dimensional feature vector  $g$ .

This feature  $g$ , at timestep  $t$  is then fed into the core network  $f_h$  which is basically an RNN (*Recurrent Neural Network*). We choose the RNN for our task, since it can memorize the prior patch information. The memorization of previous patch information is crucial due to its impact on the current time step to find the next patch. The basic RNN unit, employed here is GRU (*Gated Recurrent Unit*) [9]. We choose GRU instead of LSTM (*Long Short-Term Memory*) due to its simplicity with similar performance gain for our task. GRU also attains lower computational cost owing to have only 1 internal state, and 2 gates with fewer parameters, whereas LSTM has 2 internal states and 3 gates with more parameters. Our core network  $f_h$  consists of 512 GRU units. The current hidden state  $h_t$  of RNN at timestep  $t$  is a function of ResNet-produced feature  $g_t$  and previous state  $h_{t-1}$ . It can be written using GRU gates as follows.

$$\begin{aligned}
 h_t &= f_h(h_{t-1}, g_t) \\
 \text{or, } h_t &= \Gamma_u * c_t + (1 - \Gamma_u) * h_{t-1} \\
 \text{where, } \Gamma_u &= \sigma(\text{linear}(h_{t-1}, g_t)); \\
 c_t &= \tanh(\text{linear}(\Gamma_r * h_{t-1}, g_t)); \\
 \Gamma_r &= \sigma(\text{linear}(h_{t-1}, g_t))
 \end{aligned} \tag{1}$$

Here,  $\Gamma_u$  and  $\Gamma_r$  are two gates of GRU, i.e., *update* and *relevant* gates, respectively. Two types of activation functions, *sigmoid* ( $\sigma$ ) and *tanh* are used in GRU. The  $\text{linear}(\bar{v})$  represents a linear transformation of a vector  $\bar{v}$ ; i.e.,  $\text{linear}(\bar{v}) = W\bar{v} + B$ , where,  $W$  is a weight matrix and  $B$  is a bias vector.

Now, the  $h_t$  is embedded to  $f_i$  to predict an idiosyncratic score with respect to a textual patch. The  $f_i$  contains a regression layer to generate a scalar-valued idiosyncratic score  $i_t$ , i.e.,  $i_t = f_i(h_t)$ . Here, the concept of linear regression on the top of a deep architecture is adopted [25]. The mean-squared-error is employed here as a loss function to train  $f_i$ , and the gradient is backpropagated through  $f_h$  and  $f_g$ . The idiosyncratic score  $i_t$  is used latter for reward shaping during reinforcement learning.

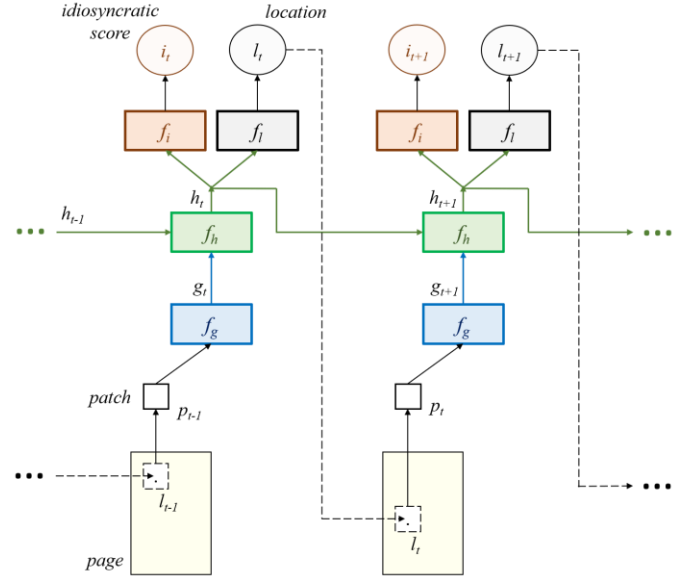


Figure 3. Idiosyncratic patch detection.

The  $h_t$  is also fed to  $f_j$  for obtaining the next patch location  $l$ . In  $f_j$ , the policy for the location  $l$  is decided by a 2-component Gaussian with a fixed variance [20]. The  $f_j$  produces the mean of the location policy at time  $t$ , and is described as  $f_j(h_t) = \text{linear}(h_t)$ . Here  $h_t$  denotes the state of the core network RNN. The  $f_j$  is trained with reinforcement learning to localize the next patch to focus.

In reinforcement learning, an agent interacts with the *state* ( $s$ ) of an environment and takes *action* ( $a$ ) to obtain the *reward* ( $r$ ) from the environment [5]. In our task, the reward is generated internally at each time step  $t$  instead of any environmental external reward. The state  $s_t$  at  $t$  takes patch input  $p_{t-1}$  and summarized into internal state  $h_t$  of RNN. The action  $a_t$  at  $t$  is actually the location-action  $l_t$  selected stochastically from a distribution  $\theta_t$ -parameterized by  $f_j(h_t)$  at  $t$ . In other words, the *state* is the patches seen so far, and the *action* is  $(x,y)$  co-ordinate of the center of the next patch to be looked at.

For reward shaping, we propose an internal reward ( $r_t$ ), generated from the idiosyncratic score  $i_t$ , as follows.

$$\begin{aligned}
r_t &= i_t; && \text{when } i_t - i_{t-1} \geq T_{r1}, i_t > T_{r2} \\
&= -(1 - i_t); && \text{when } i_t - i_{t-1} < T_{r1}, i_t > T_{r2} \\
&= -i_t; && \text{otherwise}
\end{aligned} \quad (2)$$

where,  $T_{r1} > 0$  and  $T_{r2} > 0$  are two thresholds.

Here, a positive internal reward ( $r_t$ ) is provided, if the idiosyncratic score ( $i_t$ ) at current timestep  $t$  has increased sufficiently from the score ( $i_{t-1}$ ) of previous timestep  $t-1$ . For all other cases, we put a negative internal reward. For our task,  $T_{r1} = 0.1$  and  $T_{r2} = 0.5$  works well, that are set empirically.

In reinforcement learning, an agent entails to learn a stochastic policy  $\pi_\theta(l_t|s_{1:t})$  with parameter  $\theta$  at each timestep  $t$ , that maps the past trajectory of environmental interactions  $s_{1:t} = p_0, l_0, p_1, l_1, \dots, p_{t-1}, l_{t-1}, p_t$  to an action distribution  $l_t$ . In our task, the policy  $\pi_\theta$  is defined by the early mentioned core network RNN, and  $s_t$  is summarized by the state of  $h_t$ . For the parametrized policy  $\pi_\theta$ , the parameter  $\theta$  is provided by the parameters  $\theta_g$  and  $\theta_h$  of the networks  $f_g$  and  $f_h$ , respectively, i.e.,  $\theta = \{\theta_g, \theta_h\}$ .

Here, the agent learns parameter  $\theta$  to find an optimal policy that maximizes the expected sum of discounted rewards ( $r$ ). Here, the cost function is as follows.

$$J(\theta) = E_{\rho(s_{1:T};\theta)} \left[ \sum_{t=1}^T \gamma^{t-1} r_t \right] = E_{\rho(s_{1:T};\theta)} [R] \quad (3)$$

where, the transition probability  $\rho$  from a state to another, depending on policy  $\pi_\theta$  is specified as follows.

$$\rho(s_{1:T}; \theta) = \prod_{t=1}^T \rho(s_{t+1}|s_t, l_t) \pi_\theta(l_t|s_t) \quad (4)$$

Here,  $T$  is the total count of time-step in an episode and  $\gamma$  is a discounted factor.

Now, we find the optimal policy  $\pi^*$  by optimizing the function parameter  $\theta$ . The optimal parameter  $\theta^*$  is defined as follows,  $\theta^* = \underset{\theta}{\operatorname{argmax}} J(\theta)$ . For finding the optimal policy, gradient ascent is used on policy parameters. Here, we borrow strategies from the reinforcement learning literature [6] as

follows.

$$\begin{aligned}
\nabla_\theta J(\theta) &= \sum_{t=1}^T E_{\rho(s_{1:T};\theta)} [R \nabla_\theta \log \pi_\theta(l_t|s_t)] \\
&\approx \frac{1}{N} \sum_{n=1}^N \sum_{t=1}^T R^{(n)} \nabla_\theta \log \pi_\theta(l_t^{(n)}|s_t^{(n)})
\end{aligned} \quad (5)$$

where,  $s^{(n)}$ 's are trajectories obtained by executing the agent on policy  $\pi_\theta$  for  $n=1, 2, \dots, N$  episodes. Here, the gradient estimator does not depend on transition probability  $\rho$ . Moreover, the  $\nabla_\theta \log \pi_\theta(l_t|s_t)$  part can be computed from the gradient of RNN with standard backpropagation [7].

The gradient estimator may suffer from high variance; therefore, variance reduction is necessary [8]. Here, variance reduction with baseline ( $b$ ) can be employed to understand whether a reward is better than the expected one. Now, the gradient estimator takes the following form.

$$\nabla_\theta J(\theta) \approx \frac{1}{N} \sum_{n=1}^N \sum_{t=1}^T (R_t^{(n)} - b_t) \nabla_\theta \log \pi_\theta(l_t^{(n)}|s_t^{(n)}) \quad (6)$$

where,  $R_t = Q^{\pi_\theta}(s_t, l_t) = E[\sum_{t \geq 1} \gamma^{t-1} r_t | s_t, l_t, \pi_\theta]$  and  $b_t = V^{\pi_\theta}(s_t) = E[\sum_{t \geq 1} \gamma^{t-1} r_t | s_t, \pi_\theta]$  are known as *Q-value function* and *value function*, respectively [8]. The *Q-value function* follows the execution of action  $l_t$ , but the *value function* does not depend on  $l_t$ . Here, we learn the baseline by reducing the mean squared error between *Q-value function* and *value function*.

Here, we adopt the idea of finding the next location through the recurrent neural network from [20]. However, our architecture of *Figure 3* is quite new, where the  $f_g, f_h, f_i$  nets are different from [20]. The proposed internal reward-generating technique induced by idiosyncratic score is also a new contribution.

From the architecture of *Figure 3*, we obtain top-scoring  $k$  number of idiosyncratic patches. Therefore, the number of timesteps ( $T$ ) in an episode equals  $k$ . We also empirically fix the number of episodes ( $N$ ) as 1000.

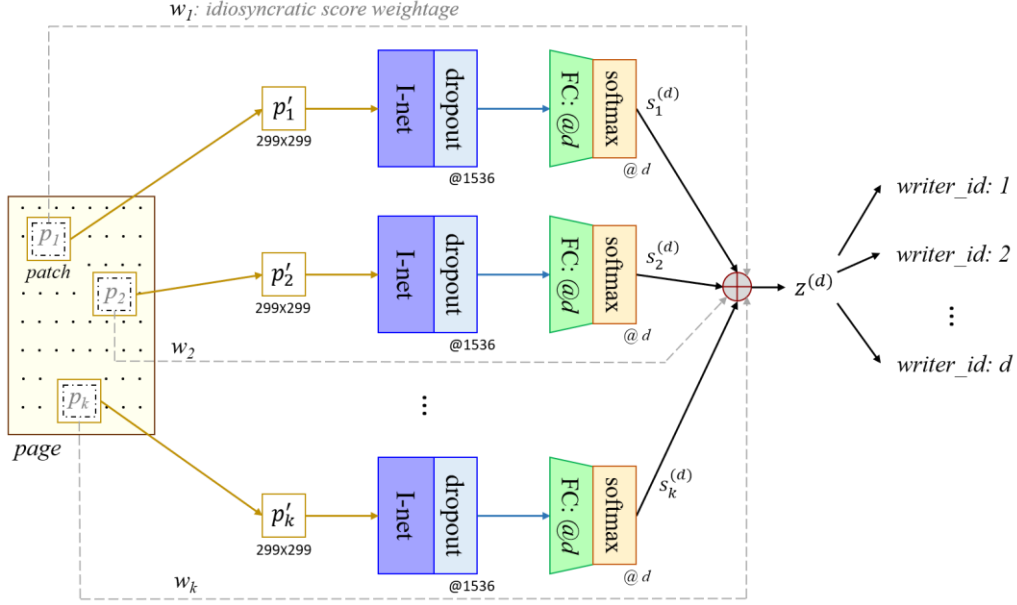


Figure 4. Writer identification architecture.

### III. WRITER IDENTIFICATION

From a handwritten page sample, we obtained  $k$  number of highly idiosyncratic patches ( $p_j$ ) that are used for writer identification. In [10], the authors showed promising outcomes from auto-derived features compared to hand-crafted features while dealing with intra-variable writing. Therefore, in this paper, we focus on obtaining auto-derived deep features. Moreover, Adak et al. [10] performed an empirical study with several state-of-the-art deep neural nets and obtained the best performance using the Xception net [11]. The contemporary Inception-ResNet-v2 architecture works better than Xception net and Inception-v4 [11, 12] on ILSVRC database [13]. Therefore, we adopt the Inception-ResNet-v2 [12] for deep feature extraction only, from a handwritten text patch. The rest of the architecture for writer inspection is our proposal.

The size of an obtained patch  $p_j$  is 224x224. We also attained the center location  $l_j$  (south-east co-ordinate among four central locations) corresponding to each  $p_j$ . From a patch  $p_j$ , we obtain  $p_j'$  of size 299x299, by the padding of the proper width. The west and north sided padding widths are of size  $[(299 - 224)/2] = 37$  each, whereas the east and south sided are of  $[(299 - 224)/2] = 38$ . Here, the padded region is filled with the original intensity values of the input page image. The reason to obtain 299x299 sized  $p_j'$  is the intention of employing some earlier layers of Inception-ResNet-v2 architecture, which takes input of size 299x299. We use up to the “average pooling” [12] layer of Inception-ResNet-v2 as a feature extractor and call it

“I-net” in the rest of this paper. Therefore, I-net produces a 1536-dimensional feature vector [12].

Now, we discuss the architecture for writer identification as shown in Figure 4. The last layer of the I-net is the “average pooling” [12] layer of Inception-ResNet-v2. After this layer, we use a dropout [14] of 20% neurons to reduce over-fitting. Next, we add a fully connected (FC) layer to obtain a feature vector of size  $d$  from each patch. Then this feature vector is transferred through a *softmax* activation function. Each patch  $p_j'$  produces a softmax probability distribution  $s_j^{(d)}$ ;  $\forall j = 1$  to  $k$ , over class labels.  $\sum_d s_j^{(d)} = 1$ . Here,  $k$  is the number of patches obtained from a page, and  $d$  is the total number of classes, i.e., the total count of writers in a database. Now, all  $s_j^{(d)}$ 's obtained from  $p_j'$ 's are combined to obtain the *writer\_id* of a page, as follows.

$$\text{writer\_id} = \underset{(d)}{\operatorname{argmax}} z^{(d)} \quad (7)$$

where,  $z^{(d)} = \frac{\sum_{j=1}^k w_j s_j^{(d)}}{\sum_{j=1}^k w_j}$ , and  $\sum_d z^{(d)} = 1$ .

Here,  $z^{(d)}$  is the weighted average of  $s_j^{(d)}$ 's. A weight  $w_j$  is associated with  $s_j^{(d)}$ . The weight  $w_j$  is determined from the idiosyncratic score ( $i_j$ ) of a patch  $p_j$  as follows.

$$\begin{aligned} w_j &= 10 \cdot i_j ; & \text{when } i_j > 0.1 \\ &= 1 ; & \text{otherwise} \end{aligned} \quad (8)$$

Here, we use *cross-entropy* [26] as the loss function due to its good performance in multi-class classification.



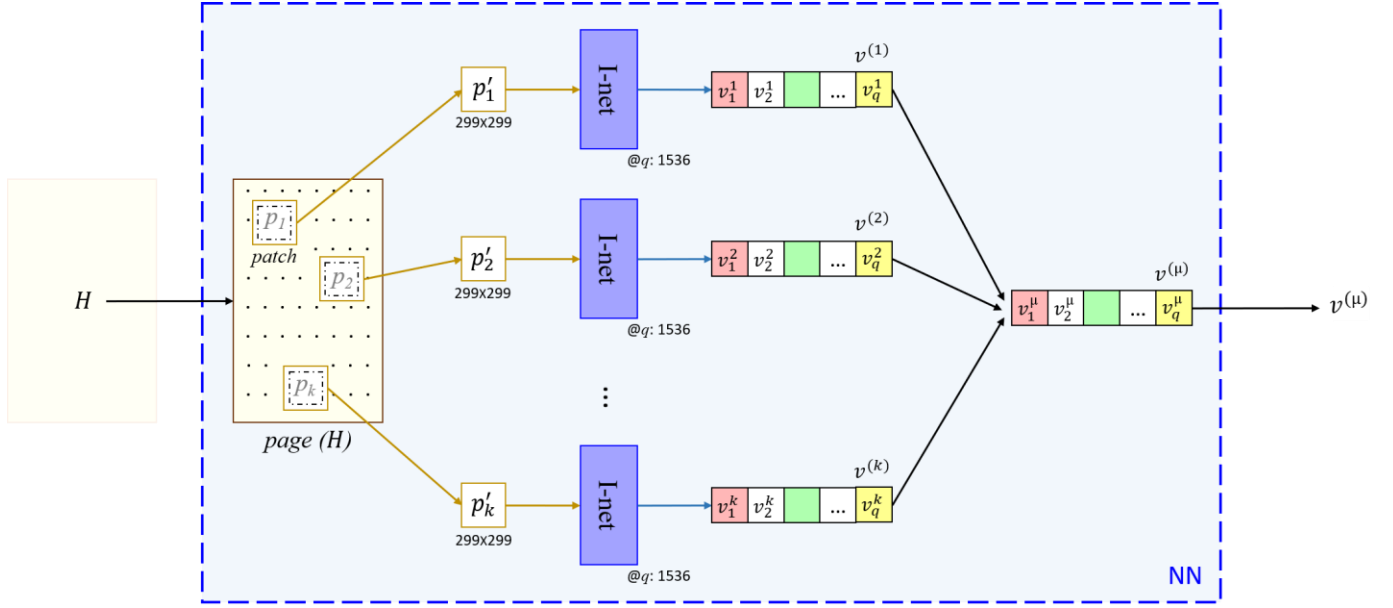


Figure 5. Feature extraction for writer verification.

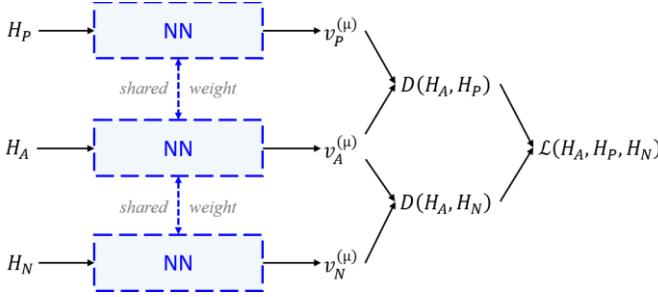


Figure 6. Triplet Network (refer to Figure 5 for NN).

#### IV. WRITER VERIFICATION

In the case of writer verification, we authenticate an unknown handwritten sample based on the samples of a known writer database. Therefore, here the task is to take input of two writing samples and produce the output either “same” if they are written by the same writer, or “different” otherwise. To measure the similarity between handwritten pages, we extract the page-level feature vectors corresponding to these pages, and compare between the feature vectors.

Here too, we use auto-derived deep features since those outperformed the handcrafted features [10]. Similar to the case of writer identification, at first, we extract  $q$  ( $=1536$ )-dimensional deep feature vectors ( $v^{(j)}: \{v_1^j, v_2^j, \dots, v_q^j\}; \forall j = 1 \text{ to } k$ ) from each of the top- $k$  idiosyncratic patches ( $p_j'$ ) using I-net (refer to Figure 5). Now, all the feature vectors  $v^{(j)}$ 's obtained from all the patches  $p_j'$ 's are aggregated to obtain a single  $q$ -dimensional feature vector ( $v^{(\mu)}: \{v_1^\mu, v_2^\mu, \dots, v_q^\mu\}$ ) corresponding to a handwritten page sample ( $H$ ). The  $v^{(\mu)}$  is calculated as follows.  $v_1^\mu = \frac{v_1^1 + v_1^2 + \dots + v_1^k}{k} = \frac{1}{k} \sum_{j=1}^k v_1^j$ ,  $v_2^\mu = \frac{v_2^1 + v_2^2 + \dots + v_2^k}{k} = \frac{1}{k} \sum_{j=1}^k v_2^j$ , ...,  $v_q^\mu = \frac{v_q^1 + v_q^2 + \dots + v_q^k}{k} =$

$\frac{1}{k} \sum_{j=1}^k v_q^j$ . In Algorithm 1 (MAF), we formally present our method to generate a *mean aggregated feature* from multiple text-patches of a handwritten page. Our MAF algorithm is different from the page-level feature generation using the *Strategy-Mean* of [10].

---

#### Algorithm 1. MAF: *page\_level\_Mean\_Aggregated\_Feature*

---

- 1: Input:  $p_j': \{p_1', p_2', \dots, p_k'\}$  | top- $k$  idiosyncratic patches in a page image  $H$ ;
  - 2: Output:  $v^{(\mu)}: \{v_1^\mu, v_2^\mu, \dots, v_q^\mu\}$  | a  $q$ -dimensional feature vector representing page image  $H$ ;
  - 3: **for**  $j=1$  to  $k$
  - 4:      $v^{(j)} = \text{I-net}(p_j')$ ;      $/*v^{(j)} := \{v_1^j, v_2^j, \dots, v_q^j\}; = \{v_x^j; \forall x = 1 \text{ to } q\}$  |  $q$ -dimensional feature vector  $*/$
  - 5: **end for**
  - 6:  $v^{(\mu)} = \text{NULL}$ ;
  - 7: **for**  $x=1$  to  $q$
  - 8:      $Sum = 0$ ;
  - 9:     **for**  $j=1$  to  $k$
  - 10:          $Sum = Sum + v_x^j$ ;
  - 11:     **end for**
  - 12:      $v_x^\mu = Sum/k$ ;
  - 13:      $v^{(\mu)} = v^{(\mu)}.append(v_x^\mu)$ ;
  - 14: **end for**
  - 15: **return**  $v^{(\mu)}$ ;
- 

In Algorithm 2 (XAF), we propose another *max aggregated feature* from multiple patches of a page. Here, the aggregated feature  $v^{(\mu)}$  is calculated as follows.  $v_1^\mu = \max(v_1^1, v_1^2, \dots, v_1^k)$ ,  $v_2^\mu = \max(v_2^1, v_2^2, \dots, v_2^k)$ , ...,  $v_q^\mu = \max(v_q^1, v_q^2, \dots, v_q^k)$ . Our XAF algorithm is different from *Strategy-Major* of [10] for page-level feature generation.

**Algorithm 2.** XAF: *page\_level\_max\_Aggregated\_Feature*


---

```

1: Input:  $p'_j: \{p'_1, p'_2, \dots, p'_k\}$  | top- $k$  idiosyncratic
   patches in a page image  $H$ ;
2: Output:  $v^{(\mu)}: \{v_1^\mu, v_2^\mu, \dots, v_q^\mu\}$  | a  $q$ -dimensional feature
   vector representing page image  $H$ ;
3: for  $j=1$  to  $k$ 
4:    $v^{(j)} = \text{I-net}(p'_j)$ ;      /*  $v^{(j)} := \{v_1^j, v_2^j, \dots, v_q^j\} :=$ 
    $\{v_x^j; \forall x = 1 \text{ to } q\}$  |  $q$ -dimensional feature vector */
5: end for
6:  $v^{(\mu)} = \text{NULL}$ ;
7: for  $x=1$  to  $q$ 
8:    $Max = v_x^1$ ;
9:   for  $j=2$  to  $k$ 
10:    if  $v_x^j > Max$ 
11:       $Max = v_x^j$ ;
12:    end if
13:  end for
14:   $v_x^\mu = Max$ ;
15:   $v^{(\mu)}.append(v_x^\mu)$ ;
16: end for
17: return  $v^{(\mu)}$ ;

```

---

Now, we have obtained a feature-vector  $v^{(\mu)}$  from a handwritten page ( $H$ ). For writer verification, we need to examine the writing style similarity/dissimilarity between pages. In other words, we measure the similarities among feature-vectors  $v^{(\mu)}$ 's representing pages  $H$ 's.

For similarity metric learning, we adopt the idea of triplet network [16], since this works better than some other similarity learning, such as Siamese net [18]. In the triplet net, three identical neural nets (NN's) produce three separate feature vectors ( $v_A^{(\mu)}, v_P^{(\mu)}, v_N^{(\mu)}$ ) from three handwritten pages ( $H_A, H_P, H_N$ ) parallelly at the same time (refer to *Figure 6*), i.e.,  $v_A^{(\mu)} = NN(H_A), v_P^{(\mu)} = NN(H_P), v_N^{(\mu)} = NN(H_N)$ . The three NN's share weights among them.

In the triplet network, we compare a *positive* sample ( $H_P$ ) and a *negative* sample ( $H_N$ ) with reference to an *anchor*/baseline sample ( $H_A$ ), simultaneously. Here,  $H_A$  and  $H_P$  handwritten samples are written by the same writer, whereas  $H_A$  and  $H_N$  samples are written by two different writers. We use Euclidean distance ( $D$ ) between  $v_A^{(\mu)}$  and  $v_P^{(\mu)}$  as a distance metric to compare  $H_A$  and  $H_P$ , i.e.,  $D(H_A, H_P) = \|v_A^{(\mu)} - v_P^{(\mu)}\|^2$ . Similarly, we compare  $H_A$  and  $H_N$  with  $D(H_A, H_N) = \|v_A^{(\mu)} - v_N^{(\mu)}\|^2$ . Finally, the wings of the triplet network are joined using a loss function, called triplet loss ( $\mathcal{L}$ ) [15] to train the similarity/dissimilarity metric. Here  $\mathcal{L}$  is defined as follows.

$$\mathcal{L}(H_A, H_P, H_N) = \max(D(H_A, H_P) - D(H_A, H_N) + \alpha, 0) \quad (9)$$

where,  $\alpha$  is a margin parameter. Empirically,  $\alpha$  is set as 0.2, when checked in the interval [0.1, 0.9] with a step of 0.1.

This triplet loss ensures that the positive sample is closer to the anchor than that of the negative one, by at least a margin  $\alpha$ .

The overall cost function ( $J$ ) of the triplet network is the sum, over the training set cardinality  $M$ , of individual losses on

different triplets, which is given as follows.

$$J = \sum_{m=1}^M \mathcal{L}(H_A^{(m)}, H_P^{(m)}, H_N^{(m)}) \quad (10)$$

Here, with reference to an anchor sample, we choose the hardest positive and hardest negative samples within a mini-batch for forming triplets [17]. This hard-triplet which is hard to train, increases the computational efficiency of the learning algorithm. The SGD (*Stochastic Gradient Descent*) with momentum is employed here for minimizing  $J$ .

In [10], a Siamese net with the contrastive loss [18] is used for writer verification. Here, we use a triplet loss-based network for writer verification, since it works better than the contrastive loss-based Siamese net [17, 18, 15].

All handwritten page pairs ( $H_i, H_j$ ) scribbled by the *same* writer are represented by  $\mathcal{P}_{same}$ , and all writing sample pairs of *different* writers are denoted as  $\mathcal{P}_{diff}$ . For system performance evaluation, we define a set of true positives ( $TP$ ) at a threshold  $t_d$ , when all writing sample pairs are correctly classified as “*same*”, i.e.,

$$TP(t_d) = \{(H_i, H_j) \in \mathcal{P}_{same}, \text{with } D(H_i, H_j) \leq t_d\} \quad (11)$$

Similarly, a set of true negatives ( $TN$ ) at  $t_d$  is defined where all pairs are correctly classified as “*different*”, i.e.,

$$TN(t_d) = \{(H_i, H_j) \in \mathcal{P}_{diff}, \text{with } D(H_i, H_j) > t_d\} \quad (12)$$

The true positive rate ( $TPR$ ) and true negative rate ( $TNR$ ) for a given writing distance  $t_d$  are defined as below.

$$TPR(t_d) = \frac{|TP(t_d)|}{|\mathcal{P}_{same}|}, \quad TNR(t_d) = \frac{|TN(t_d)|}{|\mathcal{P}_{diff}|} \quad (13)$$

The overall *accuracy* (balanced) for writer verification is calculated as follows.

$$Accuracy = \max_{t_d \in D} \frac{TPR(t_d) + TNR(t_d)}{2} \quad (14)$$

where  $t_d$  varies with a step of 0.1 in the range of  $D$ .

## V. EXPERIMENTS AND DISCUSSIONS

In this section, we discuss the experiments performed to evaluate our proposed system. We analyzed the system performance based on idiosyncratic patch detection, writer identification, and writer verification. We also compared the proposed approach with some past methods. Before proceeding to the experimental analysis, we first present the database employed for our experiments.

### A. Database Employed

For experimental analysis, we required a database (DB) containing intra-variable handwritten samples of a writer. Here, we used two databases of [10], namely *controlled* ( $D_c$ ) and *uncontrolled* ( $D_{uc}$ ) dataset. These databases are briefly discussed below.

1) *Controlled* ( $D_c$ ): This database comprises a total of 600 Bengali handwritten pages written by 100 writers, i.e., 6 pages per writer. This database contains 3 sets ( $S_f, S_m, S_s$ ) of intra-variable writing. Each of these 3 sets has 2 handwritten pages per writer. For example, a writer's handwritten sample of  $S_f$  set varies extensively with his/her writing sample of  $S_s$ .

2) *Uncontrolled ( $D_{uc}$ )*: Similar to  $D_c$ , this database contains 600 Bengali handwritten pages of 100 individuals, where each writer wrote 6 pages. However, no writer was common to  $D_c$  and  $D_{uc}$ . Here too, the database is divided into 3 sets ( $S_f$ ,  $S_m$ ,  $S_s$ ) of intra-variable writing, where each set comprises 2 pages per writer.

$D_c$  and  $D_{uc}$  are different due to their generation strategies as described in detail in [10]. Besides, there are no overlapping writers in  $D_c$  and  $D_{uc}$ .

The data of  $D_c$  and  $D_{uc}$  were augmented in [10] to train the system properly. For data augmentation, the *offline DropStroke* [10] technique was used, where some writing-strokes were dropped randomly without creating any extra stroke components. A graph-based model was used there to obtain the strokes.

After data augmentation, 22 text samples were obtained per page [10]. Each of these text samples was an input to our system. Now, each of  $S_f$ ,  $S_m$ ,  $S_s$  and  $S_f'$ ,  $S_m'$ ,  $S_s'$  sets contained 44 (=22x2) samples from each of 100 individuals.

In this paper, the experimental setup was kept similar to that in [10]. Both the databases  $D_c$  and  $D_{uc}$  were divided into training, testing, and validation set in the ratio of 2:1:1. Here,  $S_f$  set was divided into  $S_{f1}$  (training),  $S_{f2}$  (validation), and  $S_{f3}$  (testing) subsets, which contained 22, 11 and 11 handwriting samples on each of the 100 writers. As a matter of fact,  $S_f = S_{f1} \cup S_{f2} \cup S_{f3}$ . Similarly,  $S_m = S_{m1} \cup S_{m2} \cup S_{m3}$ ,  $S_s = S_{s1} \cup S_{s2} \cup S_{s3}$ ,  $S_f' = S_{f1}' \cup S_{f2}' \cup S_{f3}'$ ,  $S_m' = S_{m1}' \cup S_{m2}' \cup S_{m3}'$ ,  $S_s' = S_{s1}' \cup S_{s2}' \cup S_{s3}'$ .

### B. Idiosyncratic Patch Detection

In this subsection, we analyze our system's performance on detecting idiosyncratic patches. The proposed system predicted the idiosyncratic opinion score of a detected patch through deep regression analysis. Therefore, we used the standard performance measure for prediction, i.e., Mean Absolute Error (MAE). MAE is the arithmetic mean of the absolute differences between actual and predicted idiosyncratic opinion scores of the patches. The employed training, validation, and testing sets are discussed in the previous subsection. Some learning parameters were also tuned here.

In Table 1, we present the MAE results when  $k$  number of patches were chosen from each text sample. The results obtained from both  $D_c$  and  $D_{uc}$  databases are shown here. For  $k = 125$ , we obtained the lowest MAE of 1.03% and 1.67% for  $D_c$  and  $D_{uc}$ , respectively.

MAE focused on measuring the correctness of predicting the idiosyncratic score and did not guarantee to infer a *highly* idiosyncratic opinion score. However, in this research, we were interested in highly idiosyncratic patches for writer inspection. Therefore, we required to propose some measure which focused on analyzing highly idiosyncratic opinion score.

At this point, we proposed a performance measure, which was the arithmetic mean of normalized idiosyncratic opinion scores of  $k$  number of patches, which were obtained from each text sample. This Mean Idiosyncratic Score (MIS) inferred the detection of highly idiosyncratic patches, when the MIS was high. Here, as shown in Table 1, we obtained the highest MIS of 0.879 and 0.868 for  $D_c$  and  $D_{uc}$ , respectively, when  $k = 100$ . However, the MIS did not guarantee the correct prediction of

an idiosyncratic score. Therefore, to analyze the correctly-predicted highly idiosyncratic patch, we intended to observe both the MAE and MIS. As of Table 1,  $k=125$  produced the lowest MAE, whereas  $k=100$  produced the highest MIS. Therefore, we checked the writer-inspection performance by varying the value of  $k$  in the following subsections.

Table 1. Performance of idiosyncratic patch detection

#patches ( $k$ )	Mean Absolute Error (MAE) %		Mean Idiosyncratic Score (MIS)	
	$D_c$	$D_{uc}$	$D_c$	$D_{uc}$
50	2.08	2.96	0.618	0.610
75	1.77	1.97	0.774	0.761
100	1.30	2.08	<b>0.879</b>	<b>0.868</b>
125	<b>1.03</b>	<b>1.67</b>	0.832	0.826
150	1.75	1.86	0.783	0.779
175	2.14	2.02	0.658	0.651
200	2.85	2.98	0.595	0.593

### C. Performance of Writer Identification

In this and following subsections, we present the writer identification and verification performance of the proposed system. As stated earlier, our system was evaluated with the same experimental strategy of [10].

For writer identification/verification, a 9-tuple accuracy measure obtained from various experimental setups was used in [10]. However, among this 9-tuple, 3 elements computed the actual system performance for intra-variable handwriting inspection, i.e., training/testing on highly disparate styles of writing variability, which was termed as 3-tuple accuracy. Therefore, in this paper, we focused on this 3-tuple accuracy measure to evaluate writer identification/verification performance. The 3-tuple accuracy was ( $AE_{smv}$ ,  $AE_{sfv}$ ,  $AE_{mfv}$ ).  $AE_{smv}$  was the average accuracy obtained from experimental setups  $E_{sm}$  and  $E_{ms}$ . In  $E_{sm}$  setup, the training was performed on  $S_{s1}$  and testing was done on  $S_{m3}$ , i.e.,  $S_{s1}/S_{m3}$ , while employing  $D_c$ . The  $E_{ms}$  was the reverse experimental setup, i.e.,  $S_{m1}/S_{s3}$ , when using  $D_c$ . As a matter of fact, on  $D_{uc}$ ,  $E_{sm}$  was  $S_{s1}'/S_{m3}'$ , and  $E_{ms}$  was  $S_{m1}'/S_{s3}'$ . Similarly,  $AE_{sfv}$  and  $AE_{mfv}$  were obtained. A more detailed discussion of the experimental setup is found in [10].

During the training of our system, some learning parameters were tuned and fixed. We fixed momentum = 0.9, learning rate = 0.01, and learning rate decay =  $10^{-5}$ .

For writer identification, the standard Top-N criterion was chosen, where we computed Top-1, Top-2, Top-5 accuracy measure [10]. As mentioned earlier, the writer identification task can be seen as a multi-class classification problem and we present the results in terms of accuracy.

In Table 2, we present the Top-1 writer identification performance in terms of 3-tuple accuracy using Inception-ResNet-v2 [12] as I-net. In Table 1, we have seen that the lowest MAE and the highest MIS were obtained for  $k=125$  and  $k=100$ , respectively. Therefore, here we varied the  $k$  in a smaller span from 75 to 150 with a step of 25. Overall, we obtained the best performance for  $k=100$  on both databases  $D_c$  and  $D_{uc}$ . For  $k=125$ , overall the performance was the second-best, which was very close to the best. In general, the best 3-tuple accuracies for



$D_c$  and  $D_{uc}$  databases were (88.37%, 81.57%, 84.51%) and (87.25%, 79.67%, 82.61%), respectively. On  $D_{uc}$ , the accuracy  $AE_{sfv}$  was slightly better for  $k=125$  than while  $k=100$ . Overall, the intra-variable writer identification performance on  $D_c$  was better than  $D_{uc}$ .

Table 2. Top-1 writer identification performance

DB	#patches (k)	3-tuple accuracy (%)		
		$AE_{smv}$	$AE_{sfv}$	$AE_{mfv}$
$D_c$	75	81.72	74.83	77.92
	100	<b>88.37</b>	<b>81.57</b>	<b>84.51</b>
	125	87.75	81.21	83.83
	150	84.58	77.16	80.53
$D_{uc}$	75	81.95	74.49	78.13
	100	<b>87.25</b>	79.67	<b>82.61</b>
	125	86.74	<b>79.69</b>	82.53
	150	82.86	76.15	78.64

In general, our writer identification system performed the best when 100 patches were selected from a text sample. Therefore, in this paper, we fix  $k=100$ , for presenting the rest of the experiments on intra-variable writer identification.

In Table 3, we present Top-1, Top-2, Top-5 writer identification performances for  $k=100$  and I-net as Inception-ResNet-v2. The Top-2 measure was very close to the Top-1 performance. On  $D_c$  and  $D_{uc}$  databases, the Top-5 3-tuple accuracies were (91.54%, 84.28%, 87.18%) and (91.08%, 83.65%, 87.10%), respectively.

Table 3. Top-N writer identification performance with  $k=100$

DB	Top-N	3-tuple accuracy (%)		
		$AE_{smv}$	$AE_{sfv}$	$AE_{mfv}$
$D_c$	Top-1	88.37	81.57	84.51
	Top-2	88.63	81.84	85.01
	Top-5	91.54	84.28	87.18
$D_{uc}$	Top-1	87.25	79.67	82.61
	Top-2	88.13	80.81	83.33
	Top-5	91.08	83.65	87.10

Our writer identification architecture (Figure 4) is quite generalized, where we can employ various deep-feature generators as I-net. Apart from using the front part of the Inception-ResNet-v2 as I-net, we checked with the front part (up to “average pooling” layer) of some other powerful deep architectures, e.g., Inception-v4 [12], Xception net [11], as I-net.

In Table 4, we present the Top-1 writer identification performance with various I-nets when  $k=100$ . Here, overall, we attained the best 3-tuple accuracies (88.37%, 81.57%, 84.51%) and (87.25%, 79.67%, 82.61%) on  $D_c$  and  $D_{uc}$  databases, respectively, by employing Inception-ResNet-v2. The Inception-v4 performed similarly well, and became the second-best, overall. The Xception net also performed quite well, though secured the last rank. The Xception net performed better than some state-of-the-art deep neural nets, e.g., Inception v3, Inception v2, GoogLeNet (Inception v1), VGG-16, ResNet-101, SqueezeNet, etc. [10, 11, 1].

Table 4. Top-1 writer identification on  $k=100$  with various I-nets

DB	I-net	3-tuple accuracy (%)		
		$AE_{smv}$	$AE_{sfv}$	$AE_{mfv}$
$D_c$	Inception-ResNet-v2 [12]	<b>88.37</b>	<b>81.57</b>	84.51
	Inception-v4 [12]	88.20	81.53	<b>84.52</b>
	Xception net [11]	87.76	80.72	83.96
$D_{uc}$	Inception-ResNet-v2 [12]	<b>87.25</b>	79.67	<b>82.61</b>
	Inception-v4 [12]	87.21	<b>79.71</b>	82.53
	Xception net [11]	86.41	79.06	82.00

#### D. Performance of Writer Verification

Here also, we used the 3-tuple accuracy measure obtained from a similar experimental setup for writer identification of the previous subsection. The tuning of training parameters was also similar to the writer identification. A small difference lies in measuring the accuracy, which is discussed in Section IV.

As mentioned earlier, writer verification can be perceived as a binary classification task to decide two handwriting samples either as “same” or “different” compared to a given text sample. Here, we present the results in terms of accuracy (balanced) as given in Section IV.

For writer verification, the features obtained from the patches of a text sample was aggregated using two different algorithms, i.e., MAF (*Mean Aggregated Feature*) and XAF (*max Aggregated Feature*). We compare these two algorithms in Table 5, where we present the 3-tuple accuracy for writer verification on a varied number of patches ( $k$ ) on databases  $D_c$  and  $D_{uc}$ . Here, Inception-ResNet-v2 was used as I-net, and the triplet network was used for similarity learning.

Table 5. Writer verification performance

DB	Algo	#patches (k)	3-tuple accuracy (%)		
			$AE_{smv}$	$AE_{sfv}$	$AE_{mfv}$
$D_c$	MAF	75	88.24	80.63	85.88
		100	<b>94.87</b>	<b>86.78</b>	<b>92.12</b>
		125	94.62	86.32	91.52
		150	92.83	84.18	89.01
	XAF	75	83.76	75.59	81.72
		100	<b>90.71</b>	<b>82.47</b>	<b>87.93</b>
		125	90.49	82.21	87.18
		150	87.64	80.26	85.15
$D_{uc}$	MAF	75	84.59	79.00	83.09
		100	<b>92.45</b>	86.35	<b>90.97</b>
		125	91.76	<b>86.43</b>	90.63
		150	90.63	85.25	89.20
	XAF	75	81.78	75.40	80.19
		100	<b>88.23</b>	<b>81.86</b>	<b>86.46</b>
		125	88.05	81.34	86.17
		150	85.36	79.33	83.91

From Table 5, we observed that overall we obtained the best performance for  $k=100$  using both MAF and XAF algorithms on  $D_c$  and  $D_{uc}$ . Therefore, in this paper, we used  $k=100$  for presenting the rest of the experiments for intra-variable writer verification. Comparing MAF and XAF, we observed that MAF worked better than XAF on a various number of patches for

both the databases  $D_c$  and  $D_{uc}$ . On  $D_c$  and  $D_{uc}$ , the overall best 3-tuple accuracies were (94.87%, 86.78%, 92.12%) and (92.45%, 86.35%, 90.97%) using MAF, while  $k=100$ . In general, the intra-variable writer verification performance on  $D_c$  was better than  $D_{uc}$ .

Similar to Table 4 for writer identification, here in Table 6, we present the writer verification performance with various I-nets by employing MAF, triplet net and  $k=100$ . Here, we obtained the best 3-tuple accuracy (94.87%, 86.78%, 92.12%) and (92.45%, 86.35%, 90.97%) using Inception-ResNet-v2 on  $D_c$  and  $D_{uc}$ , respectively. The results, employing Inception-v4 were very close to the best performance.

Table 6. Writer verification on  $k=100$  with various I-nets

DB	I-net	3-tuple accuracy (%)		
		AE <sub>smv</sub>	AE <sub>sfv</sub>	AE <sub>mfv</sub>
$D_c$	Inception-ResNet-v2 [12]	<b>94.87</b>	<b>86.78</b>	<b>92.12</b>
	Inception-v4 [12]	94.71	86.34	91.83
	Xception [11]	93.66	85.19	90.05
$D_{uc}$	Inception-ResNet-v2 [12]	<b>92.45</b>	<b>86.35</b>	<b>90.97</b>
	Inception-v4 [12]	91.86	86.02	90.63
	Xception [11]	90.39	84.06	89.17

In Table 7, we present the writer verification performance with various similarity learning using MAF, Inception-ResNet-v2, and  $k=100$ . Here, the triplet network worked better than the Siamese net, and produced 3-tuple accuracies of (94.87%, 86.78%, 92.12%) and (92.45%, 86.35%, 90.97%) on  $D_c$  and  $D_{uc}$ , respectively.

Table 7. Writer verification with various similarity learning

DB	Similarity learning	3-tuple accuracy (%)		
		AE <sub>smv</sub>	AE <sub>sfv</sub>	AE <sub>mfv</sub>
$D_c$	Triplet net [16]	<b>94.87</b>	<b>86.78</b>	<b>92.12</b>
	Siamese net [18]	88.95	81.59	86.78
$D_{uc}$	Triplet net [16]	<b>92.45</b>	<b>86.35</b>	<b>90.97</b>
	Siamese net [18]	87.40	80.63	84.46

From the above experiments on writer inspection, our major observations are summarized as follows.

(i) The writer identification/verification performance on  $D_c$  database was better than on  $D_{uc}$ .

(ii) For writer identification/verification, overall, the best performance was obtained while 100 ( $=k$ ) idiosyncratic patches per text sample are used.

(iii) For writer identification/verification, the front part of the Inception-ResNet-v2 (up to “average pooling” layer) worked the best as I-net.

(iv) Overall, the writer identification/verification performances in terms of individual elements of 3-tuple accuracy in decreasing order were as follows:  $AE_{smv} > AE_{mfv} > AE_{sfv}$ .

(v) For writer verification, in general, the MAF algorithm worked better than XAF.

(vi) For writer verification, the triplet network worked better than the Siamese net during similarity learning.

## E. Comparison

In this subsection, we compare our method with past works on intra-variable handwriting. At first, we compare with respect to idiosyncrasy analysis, then writer identification followed by writer verification.

### 1. Idiosyncrasy analysis comparison:

To compare our method of idiosyncrasy analysis, we came across only one work [3] reported in the literature.

In this paper, our task is to predict the idiosyncratic score from a patch using deep regression analysis. Adak et al. [3] modeled the task into classification problem to classify the text-patches into some highly idiosyncratic classes, i.e., ID<sub>1</sub> class when normalized score  $i_t$  of patch  $p_t$  was in the interval (0.9, 1], ID<sub>2</sub> when  $i_t$  was in the range (0.8, 0.9], ID<sub>3</sub> when  $i_t$  was in (0.7, 0.8], and so on. For comparison purposes, we did a similar setting here, i.e., if  $i_t$  lied in (0.9, 1], then  $p_t$  was in class ID<sub>1</sub>, and so forth, to be in ID<sub>2</sub> and ID<sub>3</sub>. Here, if the actual score  $i_t$  of  $p_t$  was in ID<sub>1</sub>, and the regression-based predicted score ( $\neq$  actual score) of  $p_t$  was also in ID<sub>1</sub>, then the  $p_t$  was correctly classified (true positive), where the relaxed error was less than 0.1. For comparison, we calculated the accuracy (balanced) [21] from the top three idiosyncratic classes (ID<sub>1</sub>, ID<sub>2</sub>, and ID<sub>3</sub>, i.e., ID<sub>1-3</sub>), since ID<sub>1-3</sub> produced the best performance in [3]. The quantitative comparison measure by employing 100 patches from each text sample of intra-variable databases ( $D_c$  and  $D_{uc}$ ) is presented in Table 8.

Table 8. Comparison of idiosyncrasy analysis

DB	Method	Accuracy (%)
$D_c$	Adak et al. [3]	90.56
	Proposed	<b>98.35</b>
$D_{uc}$	Adak et al. [3]	89.85
	Proposed	<b>97.74</b>

In Table 8, we observe that our proposed method produced 98.35% and 97.74% accuracies on  $D_c$  and  $D_{uc}$  databases, respectively, which was better than the performance of [3].

### 2. Comparison of writer identification:

For writer identification and verification of intra-variable writing, an empirical study was presented by Adak et al. [10]. As mentioned earlier, here, we kept the similar experimental setups, employed databases, and performance measure as used in [10]. Adak et al. [10] obtained the best accuracy for their method “XN\_allo\_mean”, when compared to major state-of-the-art auto-derived feature-based deep architectures and hand-crafted feature-based support vector machines (SVMs). Therefore, we compared only with XN\_allo\_mean [10] method.

Another work of Adak et al. [3] was on analyzing idiosyncratic handwriting to identify a writer. However, they did not focus on intra-variable handwriting. Therefore, here, we were interested to test their method on our intra-variable writing’s experimental setup.

In Table 9, we compare our proposed writer identification model (employing  $k=100$ , and Inception-ResNet-v2 as I-net) with XN\_allo\_mean [10] and Adak et al. [3], in terms of Top-1 3-tuple accuracy. Our proposed model performed the best,

which attained (88.37%, 81.57%, 84.51%) and (87.25%, 79.67%, 82.61%) 3-tuple accuracies on  $D_c$  and  $D_{uc}$ , respectively. The method of Adak et al. [3] ranked the second-best, whereas the XN\_allo\_mean [10] produced the lowest result. In [10], the methods including XN\_allo\_mean did not focus on the idiosyncrasy of writing. This attests to the importance of idiosyncratic handwriting analysis for writer inspection.

Table 9. Comparison of Top-1 writer identification

DB	Method	3-tuple accuracy (%)		
		AE <sub>smv</sub>	AE <sub>sfv</sub>	AE <sub>mfv</sub>
$D_c$	Adak et al. [3]	75.42	66.75	71.04
	XN_allo_mean [10]	73.74	64.12	68.94
	Proposed	<b>88.37</b>	<b>81.57</b>	<b>84.51</b>
$D_{uc}$	Adak et al. [3]	73.68	64.07	68.84
	XN_allo_mean [10]	72.52	62.79	66.53
	Proposed	<b>87.25</b>	<b>79.67</b>	<b>82.61</b>

### 3. Comparison of writer verification:

For writer verification on idiosyncratic handwriting, the empirical study of [10] showed that XN\_allo\_mean performed better than the major state-of-the-art auto-derived feature-based deep architectures and hand-crafted feature-based SVMs, similar to the writer identification. Therefore, here also, we compared our proposed method with XN\_allo\_mean of [10] for writer verification.

The method of [3] did not tackle the writer verification problem. Therefore, we did not compare with [3] here for verification.

Our proposed method obtained the best result, when we used  $k=100$ , Inception-ResNet-v2 as I-net, MAF for feature aggregation, and triplet network for similarity learning. We compared the performance of this method with XN\_allo\_mean [10], and present the results in Table 10. It can be observed that our method worked better than XN\_allo\_mean. Here, our method attained increased (14.08%, 16.76%, 17.14%) and (12.61%, 16.55%, 16.21%) of 3-tuple accuracies on the  $D_c$  and  $D_{uc}$  databases, respectively.

Table 10. Comparison of writer verification

DB	Method	3-tuple accuracy (%)		
		AE <sub>smv</sub>	AE <sub>sfv</sub>	AE <sub>mfv</sub>
$D_c$	XN_allo_mean [10]	80.79	70.02	74.98
	Proposed	<b>94.87</b>	<b>86.78</b>	<b>92.12</b>
$D_{uc}$	XN_allo_mean [10]	79.84	69.80	74.76
	Proposed	<b>92.45</b>	<b>86.35</b>	<b>90.97</b>

From this comparative study, we observed that our method outperformed the past methods for writer inspection on intra-variable data. We also observed that idiosyncrasy analysis aided the writer identification/verification system to perform better on intra-variable handwriting.

## VI. CONCLUSION

In this paper, we worked on writer identification and verification from intra-variable handwriting. Inspecting the

writer’s scribbling on a whole page did not produce good performance. Therefore, we first planned to detect some highly idiosyncratic patches, then performed the inspection from these patches. For such patch detection, we used a recurrent reinforcement learning-based technique where the idiosyncratic score was predicted by deep feature-based regression analysis. Writer identification and verification were performed by deep neural architectures. We employed two databases  $D_c$  and  $D_{uc}$  for the experimental study. Our idiosyncrasy analyzer fostered a promising performance for the writer inspection system. For writer identification, we obtained the best Top-1 3-tuple accuracy (88.37%, 81.57%, 84.51%) and (87.25%, 79.67%, 82.61%) on the  $D_c$  and  $D_{uc}$  databases, respectively. For writer verification, our system attained the best 3-tuple accuracy (94.87%, 86.78%, 92.12%) and (92.45%, 86.35%, 90.97%) on the  $D_c$  and  $D_{uc}$  databases, respectively.

In the future, we will endeavor to generate the intra-variable writing synthetically, so that our system can learn various types of possible intra-variability of individual handwriting. Moreover, we will try to explore some implicit characteristics of handwritten strokes which may not change drastically due to intra-variability.

## REFERENCES

- [1] J. E. Costain, “Questioned Documents and the Law: Handwriting Evidence in the Federal Court System”, Journal of Forensic Sciences, vol. 22, no. 4, pp. 799-806, 1977.
- [2] M. Z. Alom et al., “The History Began from AlexNet: A Comprehensive Survey on Deep Learning Approaches”, arXiv:1803.01164, 2018.
- [3] C. Adak, B. B. Chaudhuri, M. Blumenstein, “A Study on Idiosyncratic Handwriting with Impact on Writer Identification”, Proc. Int. Conf. on Frontiers in Handwriting Recognition (ICFHR), pp. 193-198, 2018.
- [4] K. He, X. Zhang, S. Ren, J. Sun, “Deep residual learning for image recognition”, Proc. CVPR, pp. 770-778, 2016.
- [5] R. S. Sutton, A. G. Barto, “Reinforcement Learning: An Introduction”, 2<sup>nd</sup> eds., MIT Press, Cambridge, MA, 2018.
- [6] R. J. Williams, “Simple Statistical Gradient-Following Algorithms for Connectionist Reinforcement Learning”, Machine Learning, vol. 8, no. 3-4, pp. 229-256, 1992.
- [7] D. Wierstra, A. Foerster, J. Peters, J. Schmidhuber, “Solving Deep Memory POMDPs with Recurrent Policy Gradients”, Proc. Int. Conf. on Artificial Neural Networks (ICANN), pp 697-706, 2007.
- [8] R. S. Sutton, D. McAllester, S. Singh, Y. Mansour, “Policy Gradient Methods for Reinforcement Learning with Function Approximation”, Proc. NIPS, pp. 1057-1063, 1999.
- [9] K. Cho et al., “Learning Phrase Representations using RNN Encoder-Decoder for Statistical Machine Translation”, Proc. Empirical Methods in Natural Language Processing (EMNLP), pp. 1724-1734, 2014.
- [10] C. Adak, B. B. Chaudhuri, M. Blumenstein, “An Empirical Study on Writer Identification and Verification from Intra-variable Individual Handwriting”, IEEE Access, vol. 7, no. 1, pp. 24738-24758, 2019.
- [11] F. Chollet, “Xception: Deep Learning with Depthwise Separable Convolutions”, Proc. CVPR, pp. 1800-1807, 2017.
- [12] C. Szegedy, S. Ioffe, V. Vanhoucke, A. Alemi, “Inception-v4, Inception-ResNet and the Impact of Residual Connections on Learning”, Proc. AAAI, pp. 4278-4284, 2017.
- [13] O. Russakovsky et al., “ImageNet Large Scale Visual Recognition Challenge”, Int. J. Comput. Vis., vol. 115, no. 3, pp. 211-252, 2015.
- [14] N. Srivastava, G. Hinton, A. Krizhevsky, I. Sutskever, R. Salakhutdinov, “Dropout: A Simple Way to Prevent Neural Networks from Overfitting”, Journal of Machine Learning Research, pp. 1929-1958, 2014.
- [15] F. Schroff, D. Kalenichenko, J. Philbin, “Facenet: A Unified Embedding for Face Recognition and Clustering”, Proc. CVPR, pp. 815-823, 2015.
- [16] E. Hoffer, N. Ailon, “Deep Metric Learning Using Triplet Network”, Int. Workshop on Similarity-Based Pattern Recognition, pp. 84-92, 2015.
- [17] A. Hermans, L. Beyer, B. Leibe, “In Defense of the Triplet Loss for Person Re-Identification”, arXiv:1703.07737, 2017.

- [18] J. Bromley, I. Guyon, Y. LeCun, E. Säckinger, R. Shah, "Signature Verification Using A 'Siamese' Time Delay Neural Network", Proc. NIPS, pp. 737-744, 1993.
- [19] Q.H.-Thu, M.N. Garcia, F. Speranza, P. Corriveau, A. Raake, "Study of Rating Scales for Subjective Quality Assessment of High-Definition Video", IEEE Trans. on Broadcasting, vol. 57, no. 1, pp. 1-14, 2011.
- [20] V. Mnih, N. Heess, A. Graves, K. Kavukcuoglu, "Recurrent Models of Visual Attention", NIPS, pp. 2204-2212, 2014.
- [21] K. H. Brodersen, C. S. Ong, K. E. Stephan, J. M. Buhmann, "The Balanced Accuracy and Its Posterior Distribution", Proc. ICPR, pp. 3121-3124, 2010.
- [22] Y.-J. Xiong, Y. Lu, P. S. P. Wang, "Off-line Text-Independent Writer Recognition: A Survey", Int. J. of Pattern Recognition and Artificial Intelligence, vol. 31, no. 05, #1756008, 2017.
- [23] M. Bulacu, L. Schomaker, "Text-Independent Writer Identification and Verification Using Textural and Allographic Features", IEEE Trans. on Pattern Analysis and Machine Intelligence, vol. 29, no. 4, pp. 701-717, 2007.
- [24] M. Diaz, M. A. Ferrer, D. Impedovo, M. I. Malik, G. Pirlo, R. Plamondon, "A Perspective Analysis of Handwritten Signature Technology", ACM Computing Surveys, vol. 51, no. 6, article 117, 2019.
- [25] S. Lathuilière, P. Mesejo, X. A.-Pineda, R. Horaud, "A Comprehensive Analysis of Deep Regression", IEEE Trans. on PAMI, doi: 10.1109/TPAMI.2019.2910523, 2019.
- [26] I. Goodfellow, Y. Bengio, A. Courville, "Deep Learning", MIT Press, 2016.

**Chandranath Adak** (S'13, M'20) received his PhD in Analytics from University of Technology Sydney, Australia in 2019. Currently, he is employed as an Assistant Professor at Centre for Data Science, JIS Institute of Advanced Studies and Research, India. His research interests include image processing, pattern recognition, document image analysis, and machine learning-related subjects.



**Bidyut B. Chaudhuri** (F'01, LF'16) received his PhD from Indian Institutes of Technology Kanpur in 1980. He joined the Indian Statistical Institute in 1978, and retired from the regular position in 2015. Currently, he is the Pro-Vice-Chancellor (Academic) of Techno India University, West Bengal, India. His research interests include pattern recognition, machine learning, digital document processing, natural language processing, speech processing, etc.



**Chin-Teng Lin** (F'05) received his PhD in electrical engineering from Purdue University, USA in 1992. He is currently the Chair Professor of FEIT, University of Technology Sydney, Chair Professor of Electrical and Computer Engineering, NCTU, International Faculty of University of California at San-Diego (UCSD), and Honorary Professor of University of Nottingham. His research interests include computational intelligence, fuzzy neural networks, brain-computer interface, machine learning, robotics, intelligent sensing and control, etc.



**Michael Blumenstein** (SM'13) received his PhD in computational intelligence from Griffith University, Australia in 2001. He is currently a Professor and the Associate Dean (Research Strategy and Management) with the FEIT, University of Technology Sydney, Australia. His research interests include pattern recognition, artificial intelligence, video processing, document image processing, environmental science, neurobiology, coastal management, etc.

